Characterization of the Failure Behavior of Printed Circuit Boards under Dynamic Loading Conditions

P. F. Fuchs[1], Z. Major[1,2], R.W. Lang[2]
[1]*Polymer Competence Center Leoben GmbH, Leoben, A*
[2] *Institute of Materials Science and testing of Plastics, University of Leoben, A*

Abstract

Printed Circuit Boards (PCBs) are frequently exposed to a very complex combination of external and internal thermo-mechanical loads (static, cyclic and impact loads superimposed onto local and global temperature effects). Instrumented impact tests were performed in this study to characterize the failure behavior of these boards. In addition to the acceleration measurement at the impact the deformation behavior was analyzed using a high speed camera. Furthermore, monotonic fracture tests were performed on a selected model material to determine fracture toughness parameters both in terms of single and multiple fracture mechanics parameters and cohesive zone models, using two different specimen configurations. In addition to the global load-displacement curves, non-contact full-field strain analysis was performed and the near and far field strain distribution determined. Based on these measurements adequate crack tip opening displacement, crack extension data and crack tip stress values were calculated. These results will be used for further numerical simulation of the deformation and failure behavior of PCBs.

1. Introduction and Objectives

Printed circuit boards (PCBs) are frequently used in many electronic devices for a wide variety of industrial and customer applications (i.e., automotive, mobile phone). Performance and functionality of these devices highly depends on the reliability of the PCBs. As these devices are frequently also used in safety relevant applications, “failure” of these devices might cause damage with high costs and personal injury. From the perspective of the loading, PCBs are exposed to a very complex combination of external and internal thermo-mechanical loads. PCBs consist of various layers made from materials (polymers and metals) which may reveal significantly different thermo-mechanical behaviour [1]. Impact loads are of specific interest because of their frequent occurrence in PCB applications e.g. [2] [3]. In this study the impact loading situation and the subsequent crack initiation was selected for detailed analysis and discussion.

The objectives of this paper are to:

- conduct instrumented impact tests on PCBs identifying the failure modes and the loading situation.
- determine time dependent modulus values for further calculations.
- characterize the fracture behavior of a model material used for PCBs implying the calculation of fracture toughness values in terms of single (critical stress intensity factor) and multiple (crack resistance curve and cohesive zone model) parameters.

2. Experimental

While standard multilayer PCBs were used for the impact failure analysis, simplified PCBs consisting only of the glass fiber reinforced epoxy layers without copper conducting paths were used for analysis of the impact loading situation, the dynamic mechanical analysis and the fracture tests.

The characterization of the failure behavior of PCBs was performed both on component and on laboratory test specimen level. While first tests provide information about the loading of the real board and about the location of the failure, laboratory tests specimens were used to determine single and multiple fracture toughness parameters.

2.1. Impact test of PCBs

PCBs are often exposed to impact loads under service conditions. Instrumented impact tests of the PCBs were performed for characterizing the failure behavior. In addition to the acceleration measurement at the impact, the deformation behavior was analyzed using a high speed camera. The deformed board and the post-impact oscillations are shown in Fig. 1. The oscillogram was measured using the high speed camera images. Furthermore, the first maximum displacement, the frequency and the time dependent damping of the board were determined.

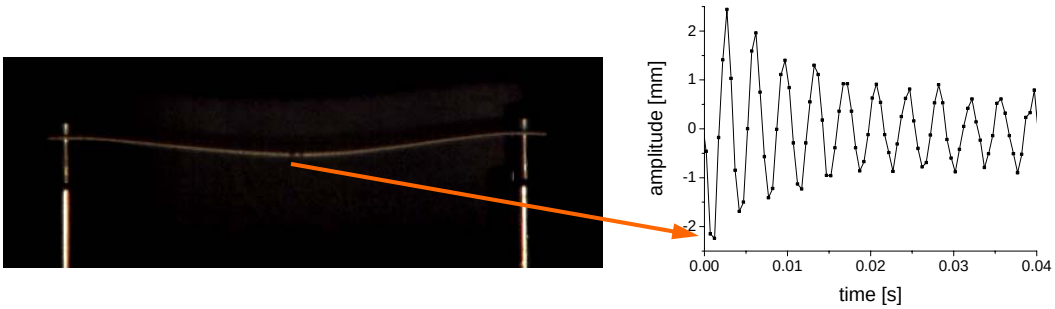

Fig. 1: High speed camera picture of the first board deflection due to the impact loading with the resulting oscillogram.

In addition to these impact tests, dynamic mechanical analysis (DMA) of the PCBs were performed over a wide frequency range using an electro dynamical tests system (BOSE 3450, BOSE Co, MN, USA) and the dynamic modulus values were determined (see Fig. 2). These time dependent modulus values will later be used for determining adequate global and local stress values. Furthermore, failure analysis of the boards tested was conducted using optical and scanning electron microscopy (SEM) and the crack initiation site was determined. A typical crack starting at the interface of the matrix and the copper filled microvia on the surface of the board is shown in Fig. 3. As the crack was observed in the polymeric matrix material further investigations were focused to characterize the fracture behavior of such materials and to determine proper fracture mechanics parameters for further numerical simulations.

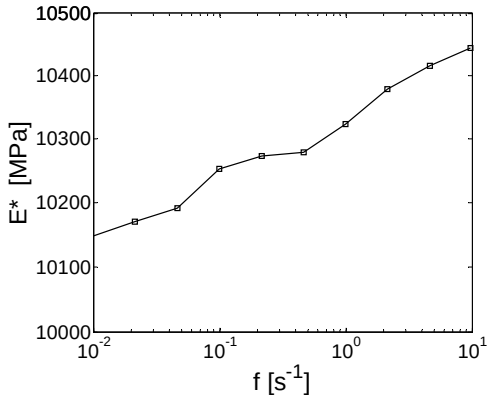

Fig. 2: Dynamic modulus, E* over frequency, f for the material investigated.

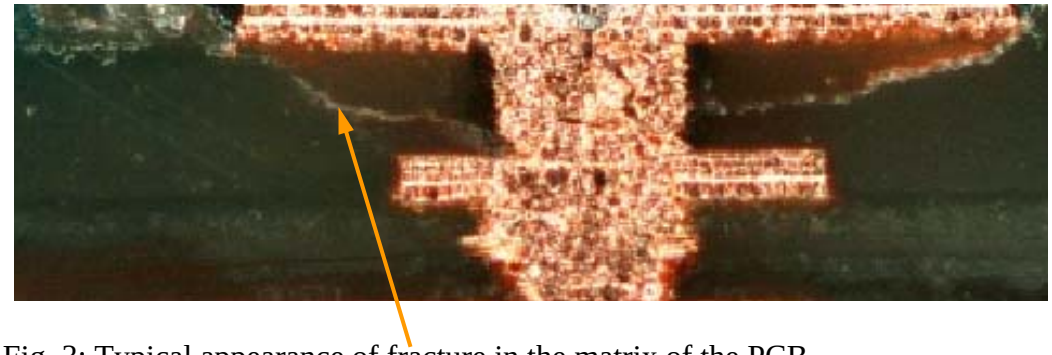

Fig. 3: Typical appearance of fracture in the matrix of the PCB.

2.2. Fracture test of materials

To determine fracture toughness parameters in terms of single and multiple fracture mechanics parameters, monotonic fracture tests were performed on a selected model material at two testing rates (10 mm/min and 100 mm/min) and using 3 different specimen configurations. The model material selected for these investigations is a multilayer glass fiber reinforced epoxy and manufactured and provided by a PCB producer.

2.3. Specimen configuration

Double edge notched tensile (DENT) and center cracked tensile (CCT) type specimens with a nominal crack length a/W-ratio of 0.5 were used in this study. A sharp notch was made by a fresh razor blade at the pre-machined crack tip. The shape and size of the specimens and the applied crack is shown in Fig. 4.

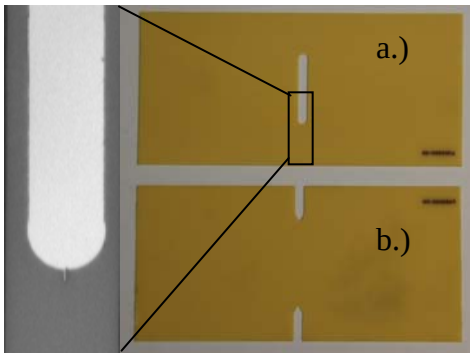

Fig. 4: The tested specimen configurations: a.) center cracked tensile (CCT)and b.) double edge notched tensile (DENT).

2.4. Determination of global load-displacement curves

A universal testing machine (Zwick Z250, Ulm, D) was used to measure global load-displacement curves (F-s). Selected load-deformation curves for the specimen configurations used are plotted in Fig. 5 at a testing rate of 100 mm/min and at room temperature.

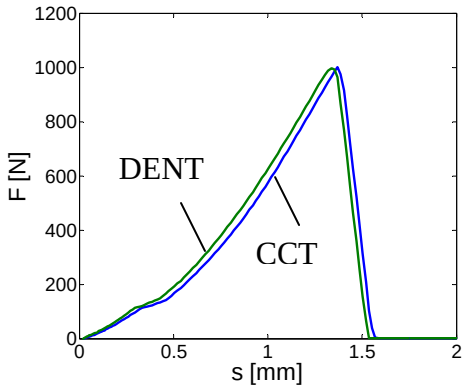

Fig. 5: Load-displacement curves (F-s) for the measured specimen configurations (blue –CCT, green- DENT).

Identical F-s curves were observed for both specimen configurations with the same nominal cross-section and crack length.

2.5. Characterization of the crack tip loading - full-field strain analysis

To gain more insight into the fracture behavior of the material full-field strain analysis was performed using a pattern image correlation system (Aramis, GOM, Braunschweig, D) at both the vicinity of the crack tip and in the specimen ligament. The local displacement field was measured and crack opening displacement (CTO) values were calculated. The full-field strain analysis image for a DENT specimen is shown in Fig. 6. The very high strain gradient at the vicinity of the crack tip can be recognized.

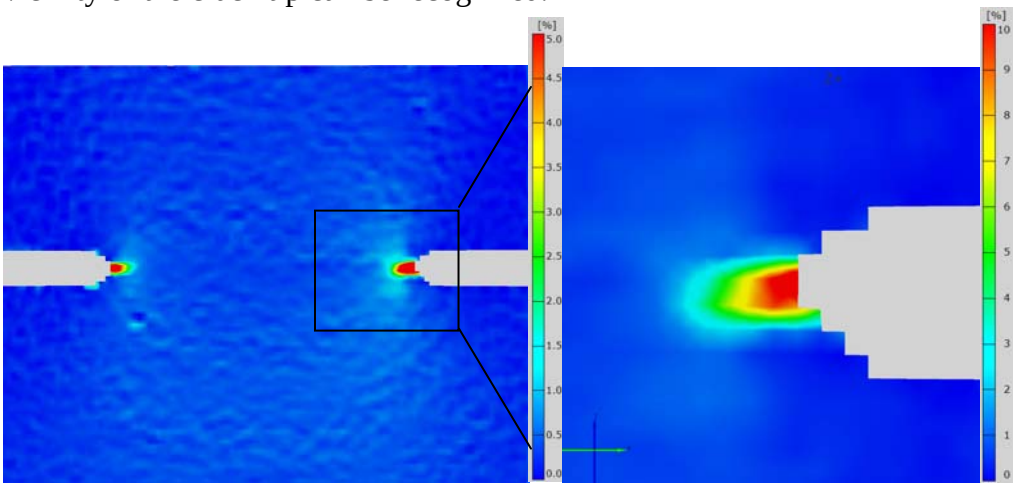

Fig. 6: Local strain values in the direction of tension measured with a pattern image correlation system.

2.6. Data Reduction

Single fracture parameters in terms of critical stress intensity factors, K_c values, were calculated based on the global measurements using the load-displacement curves. The well known equations along with specimen geometry specific geometry factors were used [4].

Furthermore, multi-point fracture parameters were calculated and crack resistance curves were constructed [5]. In this case the crack length extension, Δa, was measured during the loading and the K values have been calculated for specific crack extension values (K-Δa).

Moreover, cohesive zone type models are increasingly used to simulate fracture and debonding processes [6]. The cohesive zone model consists of the traction (stress) and local crack opening displacement (COD) values. COD values were determined using the local displacement field images. Therefore the displacement values of two symmetric lines placed tangentially to the crack process zone were subtracted (black and red line in Fig. 7.). The strain values were taken along the crack path (yellow line in Fig. 7.).

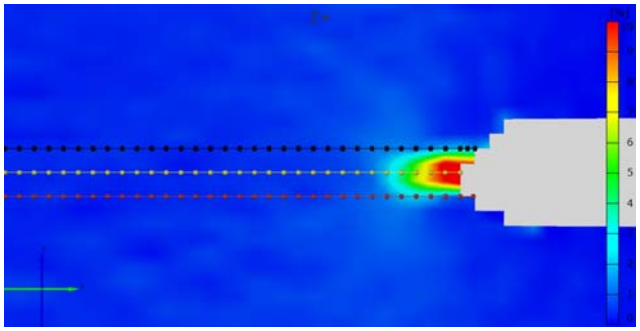

Fig. 7: Full-field strain analysis image of the DÉNT specimen with intersection lines where the values for the crack opening displacement and the local strains were determined.

To calculate the traction in the cohesive zone the J-Integral over the cohesive zone end crack opening was determined [6]. By the differentiation of this curve the cohesive stress was obtained e.g. [7 - 9].

3. Results and Discussion

In general, the selected model material revealed a brittle type fracture. The load-displacement diagrams were nearly linear up to the peak load and a sudden drop of the load was observed for DENT and CCT specimens. Fracture toughness values, K_c for the two specimen configurations are shown in Fig. 8 at two testing rates for comparison. No rate dependence and specimen configuration independence of fracture toughness values were observed.

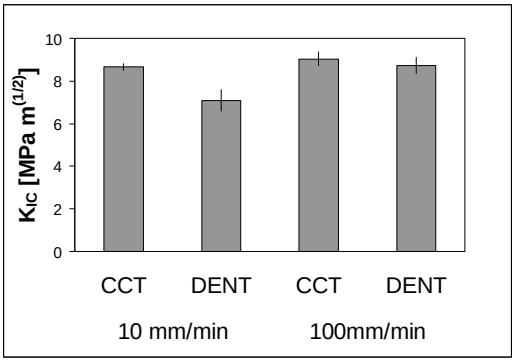

Fig. 8: Fracture toughness values for different testing rates and the different specimen configurations.

The crack resistance curves for DENT tests are shown in Fig. 9. At low loading rate the crack resistance curve is nearly horizontal up to about 4 mm crack extension and then falling. At higher loading rates the image acquisition rate of the optical system was not sufficient enough to determine reliable data.

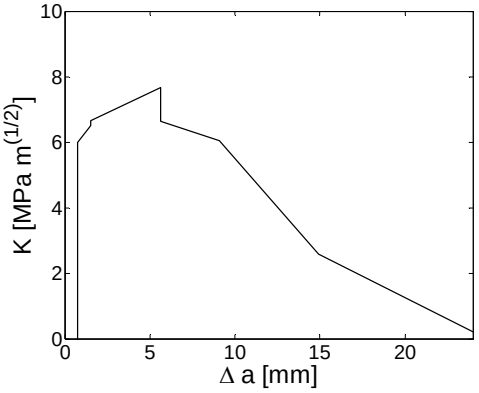

Fig. 9: Crack resistance curves of the DENT specimen at a testing rate of 10 mm/min).

The displacement values along the specimen ligament (x axis) for the upper and lower notch shoulder (Fig. 7) are shown in Fig. 10a for a DENT specimen tested at the higher load rate. The difference of these two values yields the COD values which are pictured in Fig. 10b for consecutive time steps. The red curve indicates the crack initiation. The origin of the x axis is at the center line of the specimen.

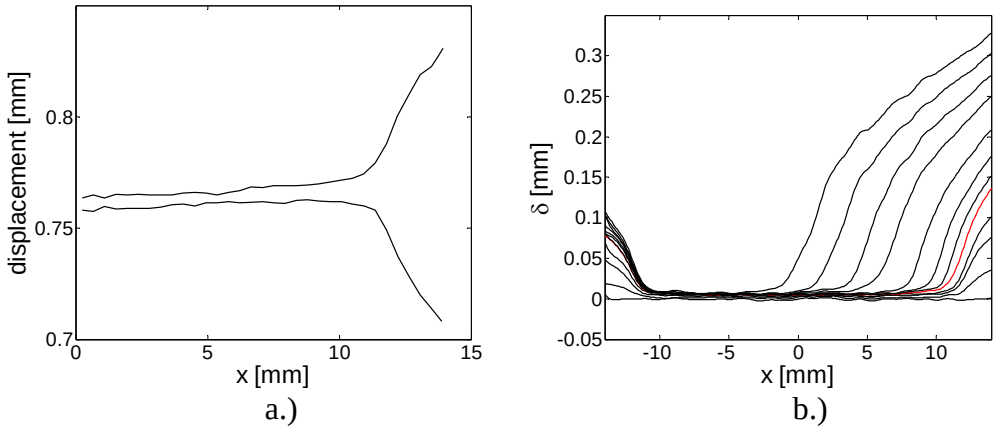

Fig. 10: a.) The displacement values for the upper and lower notch shoulder and b.) the resulting COD values at consecutive time steps. The red curve is at time of the crack initiation.

The values for the cohesive zone end opening, δ^* are determined by the evaluation of the COD values at the initial position of the crack tip (x coordinate 12 in Fig. 10b) over the time.

The J-Integral over the cohesive zone end opening is shown in Fig. 11a. The slope of this curves results in the cohesive stress, which is plotted over COD in Fig.11b. The cohesive zone law shows an increase up to a cohesive stress of about 350 MPa. Compared to that, the nominal stress calculated by the global force over

the cross sectional area is about 60 MPa. That is, the stress concentration in the cohesive zone is a factor about 6. After 0.06mm crack opening a rapid drop of the cohesive stress is observed which ends at a critical crack opening of 0.07mm. That is, the actual resulting damage zone is very small compared to the loading zone.

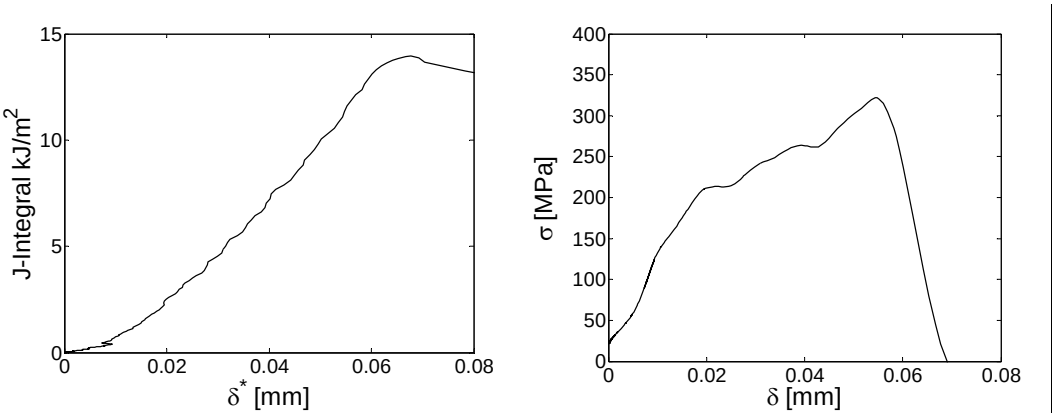

Fig. 11: a.) The J-Integral over the cohesive zone end opening and b.) the cohesive stress over the COD values.

4. Summary and Conclusions

Impact tests were carried out on PCBs and the deformation behavior including the damped oscillations was characterized. As micro-cracks were observed in the polymer matrix (see Fig. 3) the fracture behavior of an epoxy model material was investigated.

Fracture tests were performed using two various specimen configurations (CCT and DENT) on a glass fiber reinforced epoxy as model material. To determine the geometry independence single fracture toughness values, K_c, were determined. Similar fracture toughness values were obtained for the specimen configurations at two testing rates.

Furthermore, crack resistance curves, K-Δa, were also determined. While the crack resistance over the crack length was falling slowly at 10mm/min testing rate, due to the low image data acquisition rate, a not sufficient amount of images was collected to reliable determine the character of the curve for 100 mm/min.

A cohesive traction-separation law was determined for a DENT specimen applying a local full field strain measurement. The crack opening displacement was determined from the displacement field and the cohesive stresses were

calculated from the J-Integral over the cohesive zone end opening. A not pronounced damage zone is observed, which can be attributed to the unstable and very fast crack growth. However, the crack is hard to track with the camera system used and it is possible that not all the damage zone relevant data could be recorded.

Further work will focus on measurements using high frame rate cameras to determine the crack propagation. This will result in advanced crack resistance curves which will yield in a better described damage zone of the cohesive zone model.

References

[1] Ehrler S., Properties of new printed circuit board base materials: Circuit World 28/4 (2002) 38-45

[2] Jeng S.T., Sheu H.S., Yeh C.L., Lai Y.S., Wu J.D., High-G drop impact response and failure analysis of a chip packaged printed circuit board, International Journal of Impact Engineering: 34 (2007) 1655 -1667

[3] Liu F., Meng G., Zhao M., Viscoelastic influence on dynamic properties of PCB under drop impact, Journal of Electronic Packaging: 129 (2007) 266-272

[4] T.L. Anderson, Fracture Mechanics Fundamentals and Applications, Taylor and Francis Group, Boca Raton, 2005

[5] K.H. Schwalbe, J. Heerens, U. Zerbst, H. Pisarski, M. Kocak, EFAM GTP 02, GKSS-Forschungszentrum Geesthacht GmbH, Geesthacht, 2002

[6] Zhang X., Liu H.-Y., Mai Y.-W., Effects of fibre debonding and sliding on the fracture behaviour of fibre-reinforced composites, Composites: Part A 35 (2004) 1313-1323

[7] Sorensen B. F., Jacobsen T. K., Determination of cohesive laws by the J intergral approach, Engineering Fracture Mechanics: 70 (2003) 1841-1858

[8] Lindhagen J. E., Berglund L.A., Application of bridging-law concepts to short-fibre composites, Composites Science and Technology: 60 (2000) 871-883

[9] Suo Z., Bao G. and Fan. B., Delamination R-curve phenomena due to damage, Journal of the Mechanics and Physics of Solids: 40 (1992) 1-6